Numerical investigation of Tonomura experiments

1993 J. Phys. A: Math. Gen. 26 743

(http://iopscience.iop.org/0305-4470/26/3/031)

J. Phys. A: Math. Gen. 26 (1993) 743–750. Printed in the UK

Numerical investigation of Tonomura experiments

G N Afanasiev and V M Shilov

Laboratory of Theoretical Physics, Joint Institute for Nuclear Research, Dubna, Moscow District, 141980 Russia

Received 10 March 1992

Abstract. The quantitative theoretical analysis of Tonomura experiments testing the existence of the Aharonov–Bohm effect is given. The intensities of the electrons scattered by the toroidal solenoid are computed in the framework of the Fresnel–Kirchhoff diffraction theory, for different values of the magnetic flux and positions of the observation plane.

1. Introduction

A recent discussion of the Aharonov–Bohm (AB) effect is due to the fact that multivalued wavefunctions (wf) are admissible in multiconnected space regions. It turns out that literal use of mulivalued wf (that is a solution of the Schröedinger equation in terms of multivalued wf) leads to the disappearance of the AB effect. It arises only if single-valued wf are used [1]. The famous Pauli proof of wf's singlevaluedness (a very clear its exposition may be found in [2]) holds only in simply connected space regions. Thus, this ambiguity should be resolved experimentally. The earlier experiments [3] in which electrons were scattered on the cylindrical solenoid are now generally considered as insufficient. The main reasons are poor asymptotics of wf (due to the long-range behaviour of the vector potential (vp)), the non-zero return flux and the magnetic field leakages (due to the finite length of the solenoid). This allows different physical interpretations of experimental data [4, 5]. These defects are absent for the toroidal solenoid (TS). The short-range behaviour of vp ($\sim r^{-3}$ [6]) yields non-distorted asymptotics of wf. There is no return flux as the magnetic field is entirely inside TS. In the excellent experiments performed by the Japanese physicists [7] electron scattering on the impenetrable TS was studied. We shall refer to these experiments as Tonomura's experiments (TE). Now we briefly review the existing theoretical approaches. In the important paper by Luboshitz and Smorodinsky [8] the electron diffraction on TS was considered in the framework of the Frauenhofer approximation. Unfortunately, this approximation fails due to the conditions under which TE were performed. The adequate approach was developed in [9]. Based on them we aim here to give quantitative description of TE. The plan of our exposition is as follows. In section 2 the main computational formulae are presented and conditions for their validity are discussed. In section 3 the intensities of the scattered electrons are given for different values of the magnetic flux inside TS and different positions of the registration plane. In section 4 the comparison of TE with theoretical intensities is presented. In what follows we shall always use single-valued wf both in the presence or absence of magnetic fields, in simply or multiply connected space regions. As far as we know, the present treatment is the first in which AB effect for TS is analysed quantitatively, thus allowing direct comparison with experimental data.

0305-4470/93/030743+08$07.50

2. The computational formulae and their applicability

The following wf obtained in [9] describes the scattering of the plane electron wave $\exp(ikz)$ on the impenetrable TS

$$\psi = \exp(ikz) + \psi_s$$

$$\psi_s = i\frac{1+\cos\theta}{2}\exp(ikz)\exp\left(ik\frac{d^2+R^2}{2r}\right)$$

$$\times[\exp(i\omega)W_1 - \exp(2i\pi\gamma - i\omega)W_2] \qquad \gamma = e\phi/hc. \tag{2.1}$$

Here d and R are the parameters of the impenetrable torus $(\rho-d)^2+z^2=R^2$ (figure 1) with the magntic flux inside it; θ and r are the scattering angle and distance from TS to the observation point P; $\omega = k\,dR/r$, W_1 and W_2 are the linear combinations of the Lommel functions of two variables

$$W_{1,2} = U_1\left(\frac{k(d\pm R)^2}{r}, k(d\pm R)\sin\theta\right) - iU_2\left(\frac{k(d\pm R)^2}{r}, k(d\pm R)\sin\theta\right).$$

The intensity is given by the absolute square of ψ: $I=|\psi|^2$. We discuss now conditions under which (2.1) is valid. It was obtained in the framework of the Fresnel–Kirchhoff (FK) diffraction theory [10, 11]. It is suggested in this theory that wf disappears at the obstacle surface while outside it (in the plane passing through the scatterer normally to the incident wavevector) wf is approximated by the plane wave $\exp(ikz)$. This assumption (being applied to the treated case) is valid if a large number of wavelengths is confined inside the torus hole

$$k(d-R) \gg 1. \tag{2.2}$$

Then, at an arbitrary point P, wf is given by the FK diffraction integral. It reduces to (2.1) if the following additional conditions are fulfilled:

$$d \ll r \tag{2.3}$$

$$\delta \sin^2\theta \ll \pi \qquad \delta = kd^2/2r. \tag{2.4}$$

In the experiments under consideration [7, 12, 13] $d=2\times10^{-4}$ cm, $R=10^{-4}$ cm, $k=2\times10^{10}\,\mathrm{cm}^{-1}$ ($E\sim150$ keV). This gives $k(d-R)\approx2\times10^6$. Thus, (2.2) is satisfied with

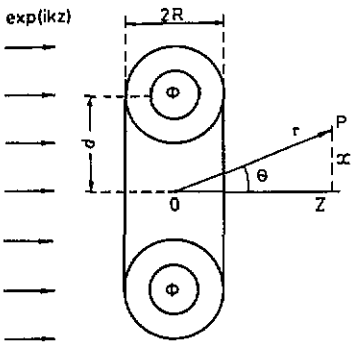

Figure 1. The schematic presentation of charged particles scattering on the impenetrable TS with the magnetic flux ϕ inside it. R and d are the parameters of TS, z and x are the position of the registration plane and the distance of the observation point from the symmetry axis of TS.

great accuracy. Numerical investigations [14] show that the FK diffraction theory works satisfactorily even if the wavelength is comparable with aperture dimensions. Special precautions were taken in TE to prevent the particle penetration into the interior of TS (where $H \neq 0$). It turns out [7] that only 10^{-6} part of the incident particles reach this region. Thus, the impenetrability condition $\psi = 0$ on the torus surface is also satisfied. Further, (2.3) is satisfied (for d given above) if r (the distance of the observation point from TS) is greater than a few parts of a millimetre. However, we did not find any information concerning r in all the available Tonomura group publications [7, 12, 13] on this subject. For definiteness, we shall study electron intensities in two $z =$ constant planes: $z = 10$ cm and $z = 100$ cm. For these there correspond values of δ equal to 4 and 0.4, respectively. Then, (2.4) leads to the following restriction on $\sin\theta$: $\sin^2\theta \leqslant \pi/4$ for $z = 10$ cm and $\sin^2\theta \ll 2\pi$ for $z = 100$ cm. In TE the measurements were performed inside the solenoid's hole ($x \leqslant d - R$) and in its close vicinity. If we take x_{max} (the maximal distance of the observation point from the TS symmetry axis) to be equal to $2(d+R) \approx 6\times10^{-4}$ cm, then $\sin\theta_{max}$ (θ_{max} is the maximal angle measured in TE) $\sim x_{max}/z$, which equals $\approx 6\times10^{-5}$ for $z = 10$ cm and 6×10^{-6} for $z = 100$ cm. Thus, inequality (2.4) is also fulfilled with great accuracy. The condition (2.2) does not mean that transition to the geometrical optics and absence of diffraction phenomena takes place. In fact, the condition (2.4) defines the angular region where Fresnel diffraction works. This is confirmed by the results of [15] in which excellent diffraction pictures were obtained. The ratio of the scatterer dimensions to the electron wavelength was of the order 10^3–10^4. The adequacy of the FK diffraction theory for the description of electron scattering is supported by thorough analysis of theoretical and experimental diffraction patterns [11].

3. Theoretical analysis of electron diffraction by toroidal solenoid

Figures 2–5 show typical electron intensities in the $z =$ constant plane. The parameters R, d and k are the same as in TE. The values of $\gamma = l\phi/he$ are taken to be 0 and $\frac{1}{2}$. This does not mean loss of generality as the theory is invariant under the shift $\gamma \to \gamma + n$ (n is an integer). Consider first the case when the distance z from the $z = 0$ plane to the registration plane is chosen to be 10 cm (figures 2 and 3). We observe a small value of electron intensity in the shadow region ($1\ \mu m \leqslant x \leqslant 3\ \mu m$). For greater distance from the z axis electron intensities are practically the same for $\gamma = 0$ and $\gamma = \frac{1}{2}$. The oscillate

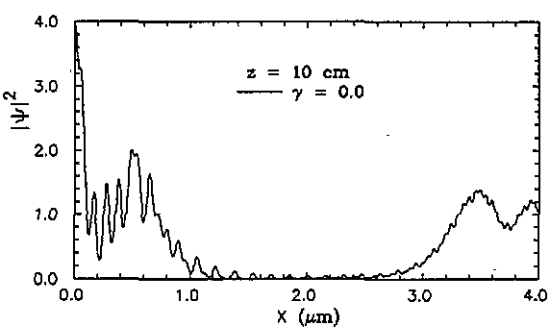

Figure 2. The intensity of scattered electrons in the $z = 10$ cm plane for the zero magnetic flux ($\gamma = e\phi/hc = 0$). The intervals $x < 1\ \mu m$ and $1\ \mu m < x < 3\ \mu m$ correspond to the torus hole and the shadow region, respectively.

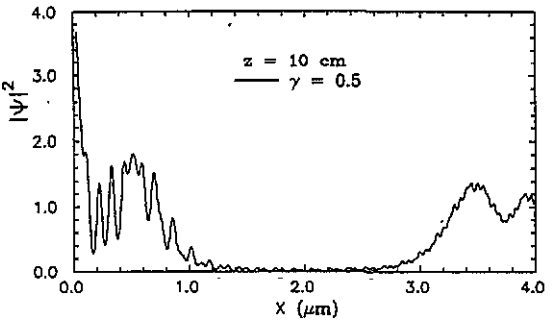

Figure 3. The same as in figure 2 but for $\gamma=\frac{1}{2}$.

around the value $|\psi|^2=1$. The amplitude of oscillations damps as x grows. For x lying inside the torus hole ($x\leqslant 1$ μm) the intensities for $\gamma=0$ and $\gamma=\frac{1}{2}$ differ appreciably (figure 4). Most of the oscillations are in a counterphase there. In figure 5 the same intensities are presented in the $z=100$ cm plane. Only one oscillation is observed inside the torus hole. The shadow region is not so strongly pronounced as in the previous case (as it should be). Figure 6 shows intensities along the z axis. In this case (2.1) is considerably simplified, and we have

$$|\psi|^2=1-8\sin\left[\frac{k(d-R)^2}{4z}\right]\sin\left(\frac{kdR}{z}-\pi\gamma\right)\cos\left[\frac{k(d+R)^2}{4z}-\pi\gamma\right]$$

We see that maxima of $|\psi|^2$ along the symmetry axis are macroscopically separated for $\gamma=0$ and $\gamma=\frac{1}{2}$. Thus, they could, in principle, be resolved experimentally.

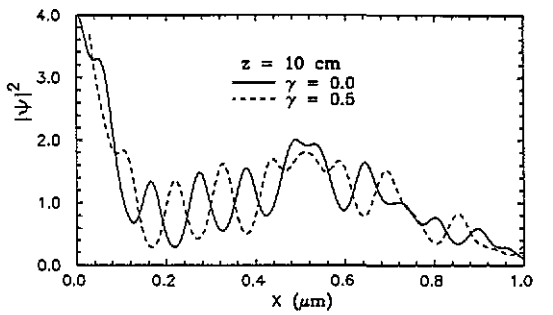

Figure 4. The intensities of two previous figures are shown inside the hole of TS.

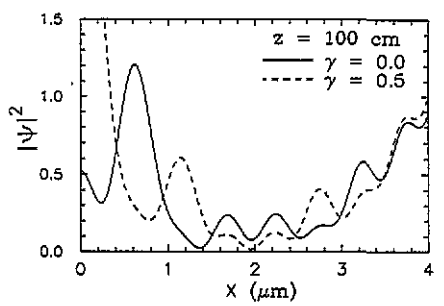

Figure 5. The intensities of scattered electrons in the $z=100$ cm plane.

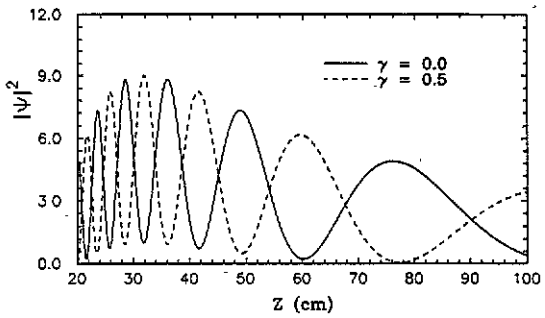

Figure 6. The electron intensities at the z axis.

4. Tonomura experiments

In the preceding section we have considered the diffraction of a plane electron wave on the impenetrable TS. However, TE were performed in a slightly different form (figure 7). An incoming electron beam is split in two parts. The first of them illuminates TS: the second part of the beam (which is referred to as a reference wave) is directed to the first part by using an electron optical system and they meet behind the TS. As a result, an interference pattern arises there, which is recorded onto photofilm. Then, using a holography method the original diffraction picture (i.e. in the absence of reference waves) is reconstructed. The experiment shows that in space region II (where ψ_{ref} interferes with the part ψ_{out} of the beam which has not passed the torus hole), the interference picture remains the same for any value of magnetic flux ϕ. In region I (where ψ_{ref} interferes with the part ψ_{in} of the beam which has passed the torus hole) the interference picture shifts with changing ϕ. The usual explanation proceeds along the following lines. Let us suggest that in the absence of the magnetic field the wf ψ_{in} and ψ_{out} may be well approximated by the plane waves: $\psi_{\text{in}} = \psi_{\text{out}} = \exp(ikt)$. Further, let the wavevector of the reference wave have the components $k_x = k \sin\alpha$ and $k_z = k \cos\alpha$. Then, $\psi_{\text{ref}} = \exp[ik(x \sin\alpha + z \cos\alpha)]$. In the absence of the magnetic field, we have in I and II: $\psi_0 = \exp(ikz) + \psi_{\text{ref}}$ and $|\psi|^2 = 2\{1 + \cos[kx \sin\alpha - kz(1 - \cos\alpha)]$. In the plane $z = \text{constant}$ (where the measurements are performed) the maxima of $|\psi_0|^2$ are at $x_n^0 = [2\pi n + kz(1 - \cos\alpha)]/k \sin\alpha$. The

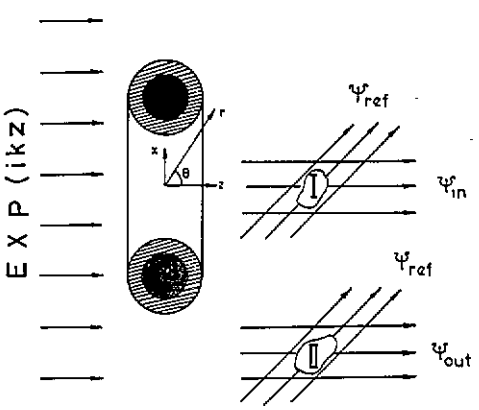

Figure 7. The schematic presentation of Tonomura experiments.

magnetic field may be taken into account by the Dirac phase factor [16]

$$\psi_{\text{in}}^{\phi} = \psi_{\text{out}}^{\phi} = \exp\left(\frac{ie}{\hbar e}\int_{-\infty}^{z} A_z(x, z)\right)\exp(ikz).$$

Here A_z is vp of TS. In spite of the same functional form this factor is different for ψ_{in}^{ϕ} and ψ_{out}^{ϕ} due to different values of x (see figure 1). Due to the short-range behaviour of A_z (at large distances $A_z \sim r^{-3}$ [6] the upper integration limit may be changed to $+\infty$. As $\int_{-\infty}^{\infty} A_z\,dz$ equals ϕ if the integration axis passes through the solenoid's hole and zero otherwise, then $\psi_{\text{out}} = \exp(ikz)$ and $\psi_{\text{in}} = \exp(ikz)\exp(2i\pi\gamma)$. This means that in space region II the interference picture remains the same as in the absence of the magnetic field, while in region I: $|\psi_I^{\phi}|^2 = 2\{1+\cos[kx\sin d - kz(1-\cos\alpha) - 2\pi\gamma]\}$. The maxima of $|\psi_I^{\phi}|^2$ are at $x_n^{\phi} = x_n^0 + 2\pi\gamma/k\sin\alpha$, that is the switching on of the magnetic field shifts them onto $\Delta = 2\pi\gamma/k\sin\alpha$. Due to the periodicity of $|\psi_I^{\phi}|^2$ w.r.t. γ it follows that it is enough to consider $0 < \gamma < 1$. Thus, the largest difference in the interference pictures takes place for $\gamma = \frac{1}{2}$.

To obtain quantitative results we superpose wf ψ given by (2.1) with ψ_{ref}. In the paper by Tonomura *et al* [12] the incidence angle α has been estimated to be 10^{-3} rad. For this value of α and $z = 10$ cm the computed interference picture is presented in figure 8. Notice the scale on the horizontal axis: the interference picture shown is displayed at the distance 10^{-2} μm. From this figure we estimate the distance between successive maxima to be $\approx 3.2\times10^{-3}$ μm, while the shift of the interference picture (due to the magnetic field switching) equals approximately half of this value (for $\gamma = \frac{1}{2}$). This agrees with the qualitative estimates given above ($\Delta x_n^0 \approx 3.14\times10^{-3}$ μm, $\Delta \approx 1.57\times10^{-3}$ μm). In spite of the fact that intensities corresponding to the superposition of ψ_{ref} with either qualitative or quantitative wf look very similar, they lead to different physical predictions. In fact, the reconstructed picture of the quantitative consideration is described by wf (2.1). The diffraction pictures corresponding to this wf were given earlier (figures 2–6). On the other hand, the reconstruction of the qualitative wf leads to the multivalued wf described by the Dirac phase factor:

$$\psi \sim \exp(ikz)\exp(2i\pi\gamma) \qquad \text{for } x \leqslant d - R \qquad \text{and } \psi \sim \exp(ikz) \qquad \text{for } x \geqslant d + R.$$

The corresponding intensity equals 1 for these values of x. Thus, this wf cannot give a non-trivial diffraction picture. We conclude that it is the minor difference between intensities mentioned above that is responsible for the appearance (after reconstruction)

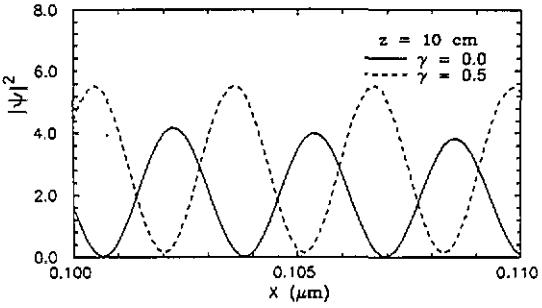

Figure 8. The intensities corresponding to the superposition of the diffracted and reference electron waves in the $z = 10$ cm plane. The incidence angle of the reference wave is $\alpha = 10^{-3}$ rad. Only part of the interference picture (0.1 μm$\leqslant x \leqslant 0.11$ μm) is shown.

of the non-trivial diffraction picture and the AB effect. From the reconstructed diffraction pictures presented in [7, 12] we estimate the distance between the neighbouring maxima $\approx 0.5\ \mu$m, while the shift of the particular maximum arising from the switching on of the magnetic field is $\approx 0.25\ \mu$m (for $\gamma = \frac{1}{2}$). On the other hand, from figures 4 and 5 of the present paper we find the diffraction pattern shift $\Delta \approx 0.06$ m for $z = 10$ cm and $\Delta \approx 0.4\ \mu$m for $z = 100$ cm. Thus, the observation plane in TE should be between these values of z. We have found that the shift of the diffraction picture observed in TE is reproduced when the distance z is chosen to be $z = 50$ cm. The corresponding diffraction picture is shown in figure 9.

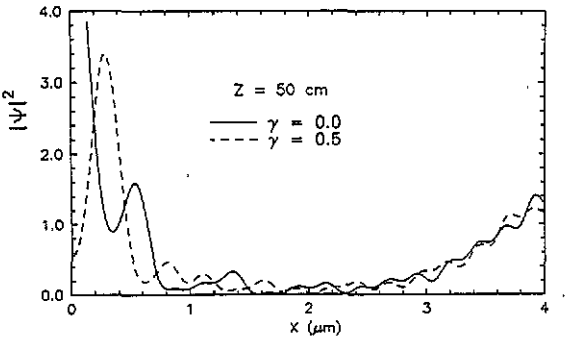

Figure 9. The intensity of scattered electrons in the $z = 50$ cm plane for which the shift of diffraction picture coincides with one observed in Tonomura experiments.

It should be noted [7, 17] that the diffraction picture observed in TE is due to the interference of a particular electron with itself (but not with another electron). In fact, the intensity of the emitted electrons in TE was so low that only one electron was inside the experimental installation at one particular instant of time.

5. Conclusion

It turns out that theoretical expressions obtained in [9] are adequate for the description of Tonomura in experiments which are the crucial ones in testing quantum mechanics. The recent communication [18] on the use of coherent point sources of low-energy (~20–50 eV) electrons should be also mentioned. According to these authors, magnification up to 150 000 times (compared with that for the plane incomming wave) may be obtained for small distances between the electron emitter and the object under investigation. This opens new possibilities for studying enclosed field effects.

References

[1] Aharonov Y 1984 *Proc. Int. Symp. Foundations of Quantum Mechanics* ed S Kamefuchi (Tokyo: Japan Phys. Soc.) pp 10–19
Yang C 1984 *Proc. Int. Symp. Foundations of Quantum Mechanics* ed S Kamefuchi pp 5–9
[2] Merzbacher E 1962 *Am. J. Phys.* **30** 237
[3] Olariu S and Popescu I 1985 *Rev. Mod. Phys.* **57** 339
[4] Berry M V 1980 *Eur. J. Phys.* **1** 154
[5] Rujsenaars S N M 1983 *Ann. Phys.* **146** 1

[6] Afanasiev G N 1987 *J. Comput. Phys.* **69** 196; 1990 *J. Phys. A: Math. Gen.* **23** 5755
[7] Peshkin M and Tonomura A 1989 *The Aharonov–Bohm Effect* (Berlin: Springer)
[8] Luboshitz V L and Smorodinsky J A 1978 *Zh. Eksp. Teor. Fiz.* **75** 40
[9] Afanasiev G N 1989 *Phys. Lett.* **142A** 222
Afanasiev G N and Shilov V M 1989 *J. Phys. A: Math. Gen.* **22** 5195
[10] Born M and Wolf E 1980 *Principles of Optics* (Oxford: Pergamon)
[11] Komrska J 1971 *Advances in Electronics and Electron Physics* vol 30 (New York: Academic) pp 139–234
[12] Tonomura A, Osakabe N, Matsuda T, Kawasaki T, Yano S and Yamada H 1986 *Phys. Rev.* A **34** 815
[13] Tonomura A, Yano S, Osakabe N, Matsuda T, Yamada H, Kawasaki T and Endo J 1987 *Proc. 2nd Int. Symp. Foundations of Quantum Mechanics* ed M Namiki, Y Ohnuki, Y Murayama and S Nomura (Tokyo: Japan Phys. Soc.) pp 97–105
Tonomura A 1988 *Physics* **151B** 206
Tonomura A 1989 *Int. J. Mod. Phys.* B **3** 521
Tonomura A 1992 *Adv. Phys.* **41** 59
[14] Silver S 1962 *J. Opt. Soc. Am.* **52** 131
[15] Matteucci G 1990 *Am. J. Phys.* **58** 1143
[16] Berry M V 1980 *Eur. J. Phys.* **2** 240
[17] Tonomura A, Endo J, Matsuda T and Kawasaki T 1989 *Am. J. Phys.* **58** 117
[18] Fink H W, Stocker W and Schmid H 1990 *Phys. Rev. Lett.* **65** 1204